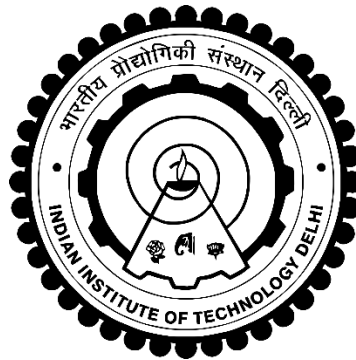


STATIC AND DYNAMIC STABILITY ANALYSES OF VARIABLE STIFFNESS COMPOSITE PANELS

MEHNAZ RASOOL



**DEPARTMENT OF APPLIED MECHANICS
INDIAN INSTITUTE OF TECHNOLOGY DELHI
SEPTEMBER 2019**

©Indian Institute of Technology Delhi (IITD), New Delhi, 2019

STATIC AND DYNAMIC STABILITY ANALYSES OF VARIABLE STIFFNESS COMPOSITE PANELS

by

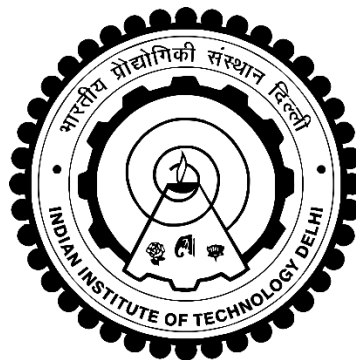
MEHNAZ RASOOL

Department of Applied Mechanics

Submitted

in fulfilment of requirements for the degree of Doctor of Philosophy

to the



INDIAN INSTITUTE OF TECHNOLOGY DELHI

SEPTEMBER 2019

Dedicated to

My sister Late Ms. Masroora Rasool and grandfather Late Mr. M. Ibrahim

CERTIFICATE

This is to certify that the thesis entitled, “*Static and Dynamic Stability Analyses of Variable Stiffness Composite Panels*” submitted by **Mr. Mehnaz Rasool** for the award of degree of **Doctor of Philosophy** to the Indian Institute of Technology Delhi is a record of bonafide research work carried out by him under my guidance and supervision.

Mr. Mehnaz Rasool has fulfilled all the prescribed requirements and the thesis is, in my opinion, worthy of consideration for the degree of Doctor of Philosophy in accordance with the regulations of the Institute. The contents of this thesis have not been submitted in part or in full to any other university or institute for the award of any degree or diploma.

Dr. M. K. Singha

Professor

Department of Applied Mechanics

Indian Institute of Technology Delhi

New Delhi-110016

India

Place: New Delhi

Date:

ACKNOWLEDGMENTS

It is not a fair task to acknowledge all the people who made this Ph.D. thesis possible with a few words. First of all, many thanks to “THE ALMIGHTY ALLAH” without His will I would have never found the right path. His mercy was with me throughout my life and ever more in this study.

I don't have the words to acknowledge my supervisor enough. I owe a debt of gratitude to **Prof. M. K. Singha** for his continuous guidance and mentorship which has molded me. This work would not have been possible without his guidance and support. His wisdom, knowledge and commitment to the highest standards have always inspired and motivated me. Prof. Singha's suggestions and problem-solving ability never let me stuck during my research work. He is not only a good researcher but also a person with full of positive energy which cultivated the seed of hope in me at every tough situation I faced throughout this work.

Beside my supervisor, I would also like to thank my student research committee members – Prof. Ajeet Kumar, Prof. Suresh Bhalla, Prof. S. Pradyuma and Prof. Santosh Kapuria for their valuable suggestions and comments throughout the research work.

I sincerely thank Prof. Arghya Samanta and Prof. Vikrant Tiwari for their advice and words of wisdom. I am highly indebted to Prof. Samanta for his much needed help. I would also like to acknowledge the INSPIRE division of Department of Science and Technology, Govt. of India for the financial assistance to carry out this research.

I am highly thankful to Prof. A. Ali, Prof. M. A. Haider and Prof. S. M. Ishtiaque and their families for the support and encouragement during the tough times.

I would like to acknowledge the support of my friends Danish, Amit, Rahman and Arif in the most difficult phase of my Ph.D and helped me to maintain the positive mindset. I am thankful to my colleagues Gaurav, Gargi, Adnan, Babu, Anurag, Bashir, Purnashis, Sriram, Hassan, Anoop, Wahi, Yadwinder, Ankita and Rishabh. Special thanks to Mayank Jain and Farooq Ahmad.

I wish to acknowledge the support of my friends Khalid Muzaffar, Tahmeed Aijaz, Tasaduq Hussain, Shahid, Zamir, Irfan, Saleem, Iliyas, Omais, Janib, Kaisar, Aamir, Omer, Mudasir, Nadeem, Zarkab and Danish, from other departments as well.

Finally, I owe my deepest gratitude and sincere appreciation to my parents for their emotional support, blessings, and encouragement throughout the work. They encouraged me at every step by investing their considerable time and never doubted on my ability to complete the task. I needed it the most and I will forever be grateful to them.

Mehnaz Rasool

ABSTRACT

The increasing demand of *lightweight structural panels* in aircrafts, spacecrafts, automobiles and civil engineering structures has necessitated the use of laminated composite materials. The curvilinear fibers, with spatially varying fiber orientation according to the requirement, may be used to design the variable stiffness composite laminates (VSCL) and reduce the weight of such panels. Hence, the structural performance of such lightweight VSCL panels is a subject of ongoing research. An attempt is made in this thesis to investigate the *stability behavior of lightweight structural panels* under various static or dynamic loading conditions using the shear deformable finite element method and the appropriate solution algorithm.

The buckling and postbuckling resistance of isotropic and laminated composite (made of straight and curvilinear fibres) shear panels is studied at the beginning. The effects of in-plane boundary conditions on the *pre-buckling state-of-stress* (associated development of a tension / *compression strip*) and out-of-plane restraints against bending / torsion of the edges on the shear buckling loads of isotropic rectangular plates are examined. Buckling loads of laminated composite plates are studied with an attempt to correlate the fibre orientation with the *compression strip*. Limited parametric study has been conducted to examine the postbuckling behavior of perfect, imperfect and eccentrically loaded thin rectangular plates with various practical boundary conditions.

Next, the dynamic stability characteristics of variable stiffness composite plates under periodic in-plane loads are taken up for investigation. The *modal transformation technique* is used to reduce the equations of motion for the flexural vibration problem of a rectangular panel into a set of Mathieu-Hill equations and the *method of multiple scales* is used to identify the dynamic instability regions. The *multi-modal response* of the shear

panels under periodic edge traction is demonstrated through the time history analysis of the coupled Mathieu-Hill equations. Thereafter, the possibility for single-mode flexural vibration (for the case of decoupled Mathieu-Hill equations) or *multi-modal response* (for coupled Mathieu-Hill equations) of isotropic and composite plates is explored for the representative cases of in-plane loading, *i.e.*, periodic compression or shear. The destabilizing zones of the excitation frequency are determined for the isotropic and composite (made of straight or curvilinear fibers) plates under in-plane compression or shear in presence or absence of static compression.

Further, the dynamic stability behaviour of variable stiffness composite laminates subjected to non-conservative compressive or shear follower loads is studied in detail. The veering of modal frequencies are studied by eigenvalue analysis to classify the divergence and flutter type of instabilities and evaluate the critical loads for isotropic and variable stiffness laminated plates under both types of follower forces. The *method of multiple scales* is used to determine the regions of instability in composite laminates under pulsating follower forces. Limited numerical examples are presented to demonstrate the simple and combination (additive / difference) type of parametric instabilities for the edge supported and cantilever panels with curvilinear fibers under compressive or shear pulsating follower forces.

Finally, the aero-elastic stability behavior of rectangular and trapezoidal VSCL panels is examined. The dynamic pressure from the high velocity airflow is evaluated from the first-order piston theory and eigenvalue analysis is performed to investigate the flutter or divergence type of instabilities in such composite panels under combined mechanical and aerodynamic loads. The limit cycle oscillation of variable stiffness plates subjected to aerodynamic pressure is investigated.

सारांश

विमान, अंतरिक्ष यान, ऑटोमोबाइल और सिविल अभियांत्रिकी संरचनाओं में हल्के संरचनात्मक पैनलों की बढ़ती मांग के कारण बहुस्तरीय कम्पोजिट का उपयोग आवश्यक हो गया है। आवश्यकता के अनुसार, स्थानिक रूप से भिन्न अभिसंकरण के साथ वक्रिय फाइबर, परिवर्तनशील कठोर बहुस्तरीय कम्पोजिट (वीएससीएल) को डिजाइन करने और ऐसे पैनलों के वजन को कम करने के लिए उपयोग किया जा सकता है। इसलिए, ऐसे हल्के वीएससीएल पैनलों का संरचनात्मक प्रदर्शन, जारी शोध का विषय है। अपप्रणव विकृति परिमित परमांश विधि और उचित समाधान कलन विधि का उपयोग करके विभिन्न स्थिर या गतिशील लोडिंग परिस्थितियों में हल्के संरचनात्मक पैनलों के स्थिरता व्यवहार की जांच करने के लिए इस थीसिस में प्रयास किया जाता है।

समदैशिक और बहुस्तरीय कम्पोजिट (सीधे और वक्राकार फाइबर से बना) अपप्रणव पैनलों के बकलिंग और पोस्टबकलिंग प्रतिरोध का शुरुआत में अध्ययन किया गया है। प्री-बकलिंग तनाव की स्थिति और अनुप्रस्थ प्रतिबंधों पर अनुदैर्घ्य सीमा स्थितियों का प्रभाव टोट्रोपिक आयताकार के अपप्रणव बकलिंग भार पर किनारों के झुकने के खिलाफ रोकता है और प्लेटों की जांच की जाती है। कम्प्रेसन स्ट्रिप के साथ फाइबर ओरिएंटेशन को सहसंबद्ध करने के प्रयास के साथ बहुस्तरीय कम्पोजिट प्लेटों की बकलिंग भार का अध्ययन किया जाता है। सीमित पैरामीट्रिक अध्ययन विभिन्न व्यावहारिक सीमा स्थितियों के साथ परिपूर्ण, अपूर्ण और विलक्षण रूप से भरी हुई पतली आयताकार प्लेटों के पोस्टबकलिंग व्यवहार की जांच करने के लिए आयोजित किया गया है।

अगला, आवधिक इन-प्लेन भार के तहत कठोर बहुस्तरीय कम्पोजिट प्लेटों की गतिशील स्थिरता विशेषताओं को जांच के लिए लिया जाता है। मोडल ट्रांसफॉर्मेशन तकनीक का उपयोग मथे-हिल समीकरणों के एक सेट में आयताकार पैनल की लचीली कंपन समस्या के लिए गति के समीकरणों को कम करने के लिए किया जाता है और गतिशील अस्थिरता क्षेत्रों की पहचान करने के लिए कई पैमानों की विधि का उपयोग किया जाता है। आवधिक बढ़त कर्षण के तहत कतरनी पैनलों की बहु-मोडल प्रतिक्रिया युग्मित मैथ्यू-हिल समीकरणों के समय के इतिहास विश्लेषण के माध्यम से प्रदर्शित की जाती है। इसके बाद, एकल-मोड फ्लेक्सुरल वाइब्रेशन (डिकॉउंटेड मैथ्यू-हिल इक्वेशन के मामले के लिए) या आइसोट्रोपिक और कम्पोजिट प्लेट्स के मल्टी-मोडल रिस्पॉन्स (कपल मैथ्यू-हिल इक्वेशन के लिए) की संभावना प्लेन लोडिंग के प्रतिनिधि मामलों के लिए पता लगाया गया है, यानी, आवधिक संपीडन या कतरनी। उत्तेजना आवृत्ति के अस्थिर क्षेत्रों को समतल

संपीडन या उपस्थिति में कतरनी या स्थैतिक संपीडन की अनुपस्थिति में आइसोट्रोपिक और समग्र (सीधे या कर्विलीनियर फाइबर से बने) प्लेटों के लिए निर्धारित किया जाता है।

इसके अलावा, गैर-रूढ़िवादी संपीडित या कतरनी अनुयायी भार के अधीन कठोर बहुस्तरीय कम्पोजिट के गतिशील स्थिरता व्यवहार का विस्तार से अध्ययन किया जाता है। मोडल फ्रिक्सेसी की वेयरिंग का अध्ययन आइजनवैल्यू विश्लेषण द्वारा किया जाता है ताकि अस्थिरता और स्पंदन प्रकार की अस्थिरताओं को वर्गीकृत किया जा सके और दोनों प्रकार की अनुयायियों बलों के तहत आइसोट्रोपिक और चर कठोरता के लिए महत्वपूर्ण भार का मूल्यांकन किया जा सके। स्पंदित अनुयायी बलों के तहत बहुस्तरीय कम्पोजिट में अस्थिरता के क्षेत्रों को निर्धारित करने के लिए कई तराजू की विधि का उपयोग किया जाता है। सीमित संख्यात्मक उदाहरण संपीडित या कतरनी स्पंदन अनुयायी बलों के तहत वक्र समर्थित और ब्रैकट पैनल के साथ किनारे के लिए पैरामीट्रिक अस्थिरता के सरल और संयोजन (योगात्मक / अंतर) प्रकार को प्रदर्शित करने के लिए प्रस्तुत किए जाते हैं।

अंत में, आयताकार और ट्रेपोजॉइडल वीएससीएल पैनलों के एयरो-लोचदार स्थिरता व्यवहार की जांच की जाती है। उच्च वेग वाले वायु प्रवाह से गतिशील दबाव का मूल्यांकन प्रथम-क्रम पिस्टन सिद्धांत से किया जाता है और संयुक्त यांत्रिक और वायुगतिकीय भार के तहत इस तरह के बहुस्तरीय पैनल में अस्थिरता या विचलन प्रकार की जांच करने के लिए आइगन वैल्यू विश्लेषण किया जाता है। वायुगतिकीय दबाव के अधीन चर कठोरता प्लेटों की सीमा चक्र दोलन की जांच की जाती है।

CONTENTS

Certificate	i
Acknowledgments	iii
Abstract	v
Contents	ix
List of Figures	xiii
List of Tables	xix
Nomenclature and Abbreviations	xxiii
CHAPTER 1	
INTRODUCTION	1
CHAPTER 2	
LITERATURE REVIEW	5
2.1 Introduction	5
2.2 Static Stability of Shear Panels	5
2.2.1 Buckling of flat panels	6
2.2.2 Postbuckling analysis of panels	7
2.2.3 Buckling and Postbuckling of Variable Stiffness Laminated Panels	9
2.3 Dynamic Stability Behaviour of Flat Panels	10
2.4 Dynamic Stability under Follower Load	14
2.5 Dynamic Stability under Aerodynamic Load	18
2.6 Summary	21
CHAPTER 3	
SCOPE AND OBJECTIVES	25
3.1 Introduction	25
3.2 Problems Considered in the Present Study	25
3.3 Analysis of Variable Stiffness Composite Panel	27

CHAPTER 4

THEORY AND FORMULATION	29
4.1 Introduction	29
4.2 Finite Element Formulation	29
4.3 Stability Analysis Under Static In-Plane Load	34
4.3.1 Postbuckling of Perfect and Imperfect Plates	35
4.4 Dynamic Stability of Shear Panels	36
4.5 Dynamic Stability of Plates under Follower Force	42
4.5.1 Solution Procedure for time-Independent Follower Force N_{xx}^F or N_{xy}^F	43
4.5.2 Solution Procedure for Periodic Follower Force $N_{xx}^F \cos \Omega t$ or $N_{xy}^F \cos \Omega t$	44
4.6 Aeroelastic Flutter Analysis	45
4.7 Summary	47

CHAPTER 5

STATIC STABILITY OF SHEAR PANELS	49
5.1 Introduction	49
5.2 Validation and Convergence Study	49
5.3 Buckling Analysis of Shear Panels	52
5.4 Postbuckling Analysis of Shear Panels	58
5.5 Buckling and Postbuckling of VSCL Plates	67
5.6 Conclusion	70

CHAPTER 6

DYNAMIC STABILITY OF SHEAR PANELS	73
6.1 Introduction	73
6.2 Problem Definition and Assessment of FEM Code	73
6.3 Dynamic Instability under Bi-axial Compression	76

6.4	Dynamic Instability under Periodic Shear $N_{xy} \cos \Omega t$	78
6.5	Dynamic Stability of Pre-stressed Panels	90
6.6	Conclusion	95
CHAPTER 7		
STABILITY OF PANELS UNDER FOLLOWER FORCES		97
7.1	Introduction	97
7.2	Validation and Convergence Study	97
7.3	Stability under Time-Independent Follower Force	99
7.4	Stability of Panels under Periodic Follower Force	105
7.5	Conclusion	112
CHAPTER 8		
AEROELASTIC FLUTTER ANALYSIS OF PANELS		115
8.1	Introduction	115
8.2	Problem Description and Assessment of FEM Code	115
8.3	Flutter Analysis of Rectangular Panels	117
8.4	Flutter Analysis of Trapezoidal Panels	122
8.5	Conclusion	124
CHAPTER 9		
CONCLUSIONS		125
9.1	Introduction	125
9.2	Summary of the Present Work	125
9.3	Scope for Future Work	129
REFERENCES		131
List of Publications from the Thesis		149
AUTHOR BIODATA		151

LIST OF FIGURES

Fig 4.2.1.	Schematic representation of a curvilinear path followed by a fibre in variable stiffness composite plates.	30
Fig 4.2.2.	Schematic representation of a nine noded and sixteen noded plate element.	31
Fig 4.2.3.	Schematic representation of a cantilever plate under conservative and non-conservative forces.	34
Fig 5.2.1.	Postbuckling response of shear loaded angle ply $[45^0/-45^0/-45^0/45^0]$ composite plate ($\bar{N}_{xy}^{cr} = N_{xy}^{cr} a^2 / E_2 h^3$; $a/b = 1$).	51
Fig 5.3.1.	Effect of boundary condition on the distribution of in-plane stresses in rectangular isotropic plates.	53
Fig 5.3.2.	Buckling mode shapes for an isotropic square plate ($\mu = 0.3$) for different boundary conditions.	55
Fig 5.3.3.	Variation of non-dimensional shear buckling load ($\bar{N}_{xy}^{cr} = N_{xy}^{cr} a^2 / E_2 h^3$) with ply angle (α) of 4-layered angle-ply $[\alpha/-\alpha/-\alpha/\alpha]$ square plates with different boundary conditions.	56
Fig 5.3.4.	Effect of aspect ratio on the critical buckling load ($\bar{N}_{xy}^{cr} = N_{xy}^{cr} a^2 / E_2 h^3$) for various ply angles of a CFFF composite plate.	57
Fig 5.4.1.	Effect of in-plane boundary conditions on the postbuckling response of isotropic and cross-ply $[0^0/90^0/90^0/0^0]$ square plates under shear load. ($\bar{N}_{xy}^{cr} = N_{xy}^{cr} a^2 / \pi^2 D$ for isotropic and $\bar{N}_{xy}^{cr} = N_{xy}^{cr} a^2 / E_2 h^3$ for composite).	58
Fig 5.4.2.	Effect of out-of-plane boundary conditions on the postbuckling response of isotropic square plates under shear load ($\bar{N}_{xy}^{cr} = N_{xy}^{cr} a^2 / \pi^2 D$).	59
Fig 5.4.3.	The effect of eccentricity on the nonlinear behaviour of cantilever (CFFF) square plate	60

Fig 5.4.4.	Postbuckling paths of angle-ply $[45^0/-45^0/-45^0/45^0]$ laminated plates under shear load ($a/h = 100$, $\bar{N}_{xy}^{cr} = N_{xy}^{cr} a^2 / E_2 h^3$; Boundary conditions SSSS and CCCC in combination with IPBC2).	61
Fig 5.4.5.	Postbuckling response of rectangular isotropic plates under shear load ($a/h = 100$, $\bar{N}_{xy}^{cr} = N_{xy}^{cr} a^2 / \pi^2 D$; boundary conditions CFCF with IPBC2 and CFFF with IPBC3).	63
Fig 5.4.6.	Postbuckling paths of rectangular cross-ply $[0^0/90^0/90^0/0^0]$ plates under shear load ($a/h = 100$, $\bar{N}_{xy}^{cr} = N_{xy}^{cr} a^2 / E_2 h^3$; boundary conditions CFCF with IPBC2 and CFFF with IPBC3).	64
Fig 5.4.7.	Postbuckling paths of square isotropic plates under combined shear and compression ($a/h = 100$, $\bar{N}_{xy}^{cr} = N_{xy}^{cr} a^2 / \pi^2 D$).	65
Fig 5.4.8.	Variation of postbuckling response for an isotropic plate under combined shear and compression ($\bar{N}_{xy}^{cr} = N_{xy}^{cr} a^2 / \pi^2 D$).	65
Fig 5.4.9.	Nonlinear variation of drift and out-of-plane deformation with aspect ratio for an unstiffened and beam stiffened isotropic shear wall.	66
Fig 5.5.1.	Postbuckling paths of a square VSCL panels for different lamination schemes for two different boundary condition ($a/h = 100$; $\bar{N}_{xy}^{cr} = N_{xy}^{cr} a^2 / E_2 h^3$).	70
Fig 5.5.2.	Effect of aspect ratio on the postbuckling paths VSCL $[\pm (0 70)]_{2S}$ plates for two different boundary condition ($\bar{N}_{xy}^{cr} = N_{xy}^{cr} a^2 / E_2 h^3$).	70
Fig 6.2.1.	Schematic representation of VSCL rectangular panels under in-plane periodic load.	74
Fig 6.3.1.	Primary instability regions of a simply supported rectangular isotropic plate under periodic bi-axial load ($N_{xx} \cos \Omega t = N_{yy} \cos \Omega t$; $\lambda = N_{xx} a^2 / \pi^2 D$; $\bar{\Omega} = \Omega a^2 \sqrt{\rho h / D} / \pi^2$; $a/b = 1.5$; $a/h = 100$; $\bar{N}_{xx}^{cr} = N_{xx}^{cr} a^2 / \pi^2 D = 1.442$).	77

- Fig 6.4.1.** Shear buckling and vibration modes of isotropic and composite square plates ($\bar{N}_{xy}^{cr} = N_{xy}^{cr} a^2 / \pi^2 D$; $\bar{\omega}_i = \omega_i a^2 \sqrt{\rho h / D} / \pi^2$ for isotropic plates and $\bar{N}_{xy}^{cr} = N_{xy}^{cr} a^2 / \pi^2 E_2 h^3$; $\bar{\omega}_i = \omega_i a^2 \sqrt{\rho / E_2 h^2} / \pi^2$ for composite plates). 79
- Fig 6.4.2.** Dynamic instability regions (DIRS) of a simply supported isotropic rectangular panel under periodic shear load $N_{xy} \cos \Omega t$ ($\lambda = N_{xy} a^2 / \pi^2 D$; $\bar{\Omega} = \Omega a^2 \sqrt{\rho h / D} / \pi^2$; $a/b = 1.5$; $a/h = 100$). 81
- Fig 6.4.3.** Time history response of an isotropic rectangular shear panel under sinusoidal edge traction $N_{xy} \cos \Omega t$ at different excitation frequencies Ω ($a/b = 1.5$; $a/h = 100$; $N_{xy} = 0.8 N_{xy}^{cr}$). 83
- Fig 6.4.4.** Dynamic instability regions of rectangular isotropic cantilever shear panel subjected to periodic edge traction $N_{xy} \cos \Omega t$ ($a/b = 1.5$; $\lambda = N_{xy} a^2 / \pi^2 D$; $\bar{\omega}_i = \omega_i a^2 \sqrt{\rho h / D} / \pi^2$; $\bar{\Omega} = \Omega / \omega_1$; $\lambda_{cr} = 0.2947$). 84
- Fig 6.4.5.** Dynamic behaviour of a simply supported angle-ply $[45^0/-45^0/45^0/-45^0/45^0]$ composite plate under periodic edge compression $N_{yy} \cos \Omega t$ and edge traction $N_{xy} \cos \Omega t$ ($a/b = 1$; $\lambda_{cr}^c = N_{xx} a^2 / \pi^2 E_2 h^3 = 4.4145$; $\lambda_{cr}^s = N_{xy} a^2 / \pi^2 E_2 h^3 = 5.1422$; $\bar{\Omega} = \Omega / \omega_1$). 85
- Fig 6.4.6.** Dynamic instability regions (DIRS) of a simply supported VSCL $[\pm (0|70)]_{2s}$ plate under periodic edge compression $N_{xx} \cos \Omega t$ and edge shear $N_{xy} \cos \Omega t$ ($a/b = 1$; $a/h = 100$; $\bar{\Omega} = \Omega a^2 \sqrt{\rho / E_2} / \pi^2 h$). 86
- Fig 6.4.7.** Dynamic instability regions of a rectangular angle-ply $[45^0/-45^0/45^0/-45^0/45^0]$ composite plate under periodic edge traction $N_{xy} \cos \Omega t$ for various boundary conditions ($a/b = 1.5$; $\lambda = N_{xy} a^2 / \pi^2 E_2 h^3$; $\bar{\omega}_i = \omega_i a^2 \sqrt{\rho / E_2 h^2} / \pi^2$; $\bar{\Omega} = \Omega / \omega_1$). 88
- Fig 6.4.8.** Effect of boundary condition on the dynamic instability regions of a VSCL $[\pm (0|70)]_{2s}$ rectangular composite plate under periodic edge traction $N_{xy} \cos \Omega t$ ($a/b = 1.5$; $a/h = 100$; $\bar{N}_{xy}^{cr} = N_{xy}^{cr} a^2 / \pi^2 E_2 h^3$; $\lambda = N_{xy} a^2 / \pi^2 E_2 h^3$; $\bar{\Omega} = \Omega a^2 \sqrt{\rho / E_2} / \pi^2 h$). 89

- Fig 6.5.1.** Dynamic instability regions of simply supported rectangular isotropic plate subjected to static and dynamic in-plane shear ($a/b = 1.5$; $N = N_{xy0} + N_{xy} \cos \Omega t$; $\lambda_{cr} = N_{xy} a^2 / \pi^2 D = 3.4144$;
 $\bar{\Omega} = \Omega a^2 \sqrt{\rho h / D} / \pi^2$). 91
- Fig 6.5.2.** Dynamic instability regions of compressed simply supported rectangular isotropic plate subjected to periodic in-plane shear ($N = N_{xx0} + N_{xy} \cos \Omega t$ ($a/b = 1.5$; $a/h = 100$; $\bar{N}_{xx}^{cr} = 4.2732$; $\bar{N}_{xy}^{cr} = 3.4144$;
; $\lambda = N_{xy} a^2 / \pi^2 D$; $\bar{\Omega} = \Omega a^2 \sqrt{\rho h / D} / \pi^2$). 92
- Fig 6.5.3.** Dynamic instability regions of compressed simply supported rectangular angle ply $[45^0/-45^0/45^0/-45^0/45^0]$ plate subjected to periodic in-plane shear ($a/b = 1.5$; $N = N_{xx} + N_{xy} \cos \Omega t$;
 $\lambda = N_{xx} a^2 / \pi^2 E_2 h^3 = 4.504$; $\lambda = N_{xy} a^2 / \pi^2 E_2 h^3 = 3.214$;
 $\bar{\Omega} = \Omega a^2 \sqrt{\rho / E_2} / \pi^2 h$). 93
- Fig 6.5.4.** Dynamic instability regions of compressed simply supported rectangular VSCL $[\pm (0|70)]_{2s}$ plate subjected to periodic in-plane shear ($a/b = 1.5$; $a/h = 100$; $N = N_{xx} + N_{xy} \cos \Omega t$; $\bar{N}_{xx}^{cr} = 6.280$;
 $\bar{N}_{xy}^{cr} = 6.395$; $\lambda = N_{xy} a^2 / \pi^2 E_2 h^3$; $\bar{\Omega} = \Omega a^2 \sqrt{\rho / E_2} / \pi^2 h$). 94
- Fig 7.3.1.** Instability response of a square isotropic plate under compressive and shear follower load for different boundary conditions ($\varpi = \omega b^2 / \pi^2 \sqrt{\rho / D}$; $\lambda = N_{xx}^F a^2 / \pi^2 D$ for compression;
 $\lambda = N_{xy}^F a^2 / \pi^2 D$ for shear). 100
- Fig 7.3.2.** Non-dimensional flutter load ($\lambda = N_{xx}^F a^2 / \pi^2 E_2 h^3$) and frequency ($\varpi = \omega b^2 / \pi^2 \sqrt{\rho / E_2 h^2}$) for an angle ply $[\theta / -\theta / -\theta / \theta]$ constant stiffness composite plate. 101
- Fig 7.3.3.** Flutter and divergence of $[\pm (0|70)]_{2s}$ square variable stiffness composite laminate (VSCL) subjected to compressive and shear follower forces ($\varpi = \omega b^2 / \pi^2 \sqrt{\rho / E_2 h^2}$; $\lambda = N_{xx}^F a^2 / \pi^2 E_2 h^3$ for compression; $\lambda = N_{xy}^F a^2 / \pi^2 E_2 h^3$ for shear). 102

- Fig 7.3.4.** Non-dimensional flutter load and frequency for a square VSCL [\pm (30|60)]_{2S} plate with compressive and shear follower load ($\varpi = \omega b^2 / \pi^2 \sqrt{\rho / E_2 h^2}$; $\lambda = N_{xx}^F a^2 / \pi^2 E_2 h^3$ for compression; $\lambda = N_{xy}^F a^2 / \pi^2 E_2 h^3$ for shear). 103
- Fig 7.4.1.** Comparison of regions of instability of a square cantilever isotropic plate for periodic in-plane loads and periodic follower loads ($\lambda = N_{xx} a^2 / \pi^2 D$ for in-plane compression; $\lambda = N_{xx}^F a^2 / \pi^2 D$ for compressive follower; $\lambda = N_{xy} a^2 / \pi^2 D$ for in-plane shear; $\lambda = N_{xy}^F a^2 / \pi^2 D$ for shear follower; $\bar{\Omega} = \Omega a^2 \sqrt{\rho h / D} / \pi^2$; $a/h = 100$). 106
- Fig 7.4.2.** Parametric response of a VSCL [\pm (0|70)]_{2S} plate with CFSS boundary conditions under periodic follower loading ($a/h = 100$; $\lambda = N_{xx}^F a^2 / \pi^2 E_2 h^3$ for compressive follower; $\lambda = N_{xy}^F a^2 / \pi^2 E_2 h^3$ for shear follower; $\bar{\Omega} = \Omega a^2 \sqrt{\rho / E_2} / \pi^2 h$). 108
- Fig 7.4.3.** Dynamic instability regions of a VSCL [\pm (0|70)]_{2S} rectangular composite plate under periodic compressive follower load ($N_{xx}^F \cos \Omega t$) for different boundary conditions ($a/b = 1.5$; $a/h = 100$; $\lambda = N_{xx}^F a^2 / \pi^2 E_2 h^3$; $\bar{\Omega} = \Omega a^2 \sqrt{\rho / E_2} / \pi^2 h$). 109
- Fig 7.4.4.** Dynamic instability regions of cantilever VSCL [\pm (0|70)]_{2S} plate subjected to periodic follower forces ($a/b = 1.0$; $a/h = 100$; $\lambda = N_{xx}^F a^2 / \pi^2 E_2 h^3$ for compressive follower; $\lambda = N_{xy}^F a^2 / \pi^2 E_2 h^3$ for shear follower; $\bar{\Omega} = \Omega a^2 \sqrt{\rho / E_2} / \pi^2 h$). 111
- Fig 7.4.5.** Dynamic instability regions of cantilever VSCL [\pm (30|60)]_{2S} plate subjected to periodic follower forces (a) Compressive follower (b) shear follower loads ($a/b = 1.0$; $a/h = 100$; $\lambda = N_{xx}^F a^2 / \pi^2 E_2 h^3$ for compressive follower; $\lambda = N_{xy}^F a^2 / \pi^2 E_2 h^3$ for shear follower; $\bar{\Omega} = \Omega a^2 \sqrt{\rho / E_2} / \pi^2 h$). 112
- Fig 8.2.1.** Schematic representation of a variable stiffness panels under free stream air flow and in-plane loads. 116

Fig 8.3.1. Coalescence of frequencies for 8-layered simply supported 118
constant stiffness and variable stiffness composite plates

$$\bar{\omega} = \omega b^2 / \pi^2 \sqrt{\rho / E_2 h^2}$$

Fig 8.3.2. Nonlinear flutter response of a square isotropic and variable 122
stiffness composite plates for different boundary conditions
(SSSS1 is the simply supported boundary condition with
immovable edges i.e. $u_0 = v_0 = 0$ along all edges).

LIST OF TABLES

Table 2.6.1.	Literature on the buckling and postbuckling analysis of isotropic and composite (CSCL and VSCL) panels.	22
Table 2.6.2.	The research studies on the dynamic stability of plates under periodic in-plane loads using various methods.	23
Table 2.6.3.	Literature on the stability of structures subjected to follower loading.	24
Table 2.6.4.	Aeroelastic stability studies of panels under aerodynamic and various loads.	24
Table 5.2.1.	Non dimensional shear buckling load ($\bar{N}_{xx}^{cr} = N_{xx}^{cr} a^2 / \pi^2 D$ or $\bar{N}_{xy}^{cr} = N_{xy}^{cr} a^2 / \pi^2 D$) of isotropic square plate ($a/h=100$) for various assumed states-of-stress.	50
Table 5.2.2.	Postbuckling response (N_{xx} / N_{xx}^{cr}) of simply supported isotropic and composite square plates ($a/h = 100$).	51
Table 5.3.1.	Non dimensional shear buckling load $\bar{N}_{xy}^{cr} = N_{xy}^{cr} a^2 / \pi^2 D$ of isotropic square plate ($\mu = 0.3, a/h = 100$) for various boundary conditions (both in-plane and out-of-plane).	54
Table 5.5.1.	Comparison of a non-dimensional shear buckling load ($\bar{N}_{xy}^{cr} = N_{xy}^{cr} a^2 / \pi^2 D$ for isotropic and $\bar{N}_{xy}^{cr} = N_{xy}^{cr} a^2 / \pi^2 E_2 h^3$ for composite) for a simply supported square plate with two in-plane boundary conditions.	68
Table 5.5.2.	Convergence of a non-dimensional buckling load ($\bar{N}_{xx}^{cr} = N_{xx}^{cr} a^2 / \pi^2 E_2 h^3$ for compression; $\bar{N}_{xy}^{cr} = N_{xy}^{cr} a^2 / \pi^2 E_2 h^3$ for shear) for a simply supported VSCL square plate under in-plane compression and in-plane shear.	68
Table 5.5.3.	The non-dimensional buckling load ($\bar{N}_{xx}^{cr} = N_{xx}^{cr} a^2 / \pi^2 E_2 h^3$ for compression; $\bar{N}_{xy}^{cr} = N_{xy}^{cr} a^2 / \pi^2 E_2 h^3$ for shear) for a simply supported VSCL square plate under in-plane compression and in-plane shear.	69
Table 6.2.1.	Comparison of first eight non-dimensional vibration frequencies of isotropic and composite plates square plates (a/h	75

= 1000; $\bar{\omega} = \omega a^2 / \pi^2 \sqrt{\rho h / D}$ for isotropic and $\bar{\omega}_i = \omega_i a^2 \sqrt{\rho / E_2} / \pi^2 h$ for composite plates).

- Table 6.2.2.** Comparison of natural frequencies (Hz) of Clamped VSCL square ($a = b = 1$ m, $h = 0.01$ m) plate for various layer schemes ($E_1 = 173$ GPa, $E_2 = 7.2$ GPa, $G_{12} = G_{13} = G_{23} = 3.76$ GPa, $\mu_{12} = \mu_{13} = \mu_{23} = 0.29$, $\rho = 1540$ kg/m³). 76
- Table 7.2.1.** Comparison of flutter frequency and flutter load for a rectangular isotropic CFSS plate ($a/h = 100$, $\mu = 0.3$, $\omega_{cr} = \omega b^2 \sqrt{\rho / D}$ and $\lambda_{cr} = N_{xx}^F a^2 / D$) 98
- Table 7.2.2.** Comparison of flutter frequency and flutter load for a square angle ply composite CFSS plate for different lamination schemes ($a/h = 100$; $\omega_{cr} = \omega b^2 \sqrt{\rho / E_2 h^2}$ and $\lambda_{cr} = N_{xx}^F a^2 / E_2 b h^3$) 98
- Table 7.3.1.** Non-dimensional flutter frequency and flutter load for a VSCL composite plate with CFSS boundary condition for various lamination schemes and aspect ratio ($\omega_{cr} = \omega b^2 / \pi^2 \sqrt{\rho / E_2 h^2}$ $\lambda_{cr} = N_{xx}^F a^2 / \pi^2 E_2 h^3$ for compression; $\lambda_{cr} = N_{xy}^F a^2 / \pi^2 E_2 h^3$ for shear). 104
- Table 7.3.2.** Non-dimensional flutter frequency and flutter load for a VSCL composite plate with CFFF boundary condition for various lamination schemes and aspect ratio ($\omega_{cr} = \omega b^2 / \pi^2 \sqrt{\rho / E_2 h^2}$ $\lambda_{cr} = N_{xx}^F a^2 / \pi^2 E_2 h^2$ for compression; $\lambda_{cr} = N_{xy}^F a^2 / \pi^2 E_2 h^2$ for shear). 104
- Table 7.4.1.** Parametric coefficient matrices ($C_{mn} = S_{mn} \omega_m \omega_n$) for a square cantilever isotropic plate under conservative follower in-plane loads. 107
- Table 7.4.2.** Parametric coefficient matrices ($C_{mn} = S_{mn} \omega_m \omega_n$) for rectangular ($a/b = 1.5$) VSCL [\pm (0|70)]_{2s} plates. 110

Table 8.2.1.	Comparison of critical aerodynamic pressure (λ_{cr}) for square isotropic and composite plate for different boundary conditions ($a/h = 100$; $\lambda_{cr} = \lambda a^3 / D$ for isotropic and $\lambda_{cr} = \lambda a^3 / E_2 h^3$ for composite).	117
Table 8.2.2.	Comparison of non-dimensional natural frequencies $\varpi = \omega a^2 / \pi^2 \sqrt{\rho h / D}$ for a symmetric simply supported isotropic trapezoidal panel.	117
Table 8.3.1.	Critical aerodynamic pressure ($\lambda_{cr} = \lambda a^3 / E_2 h^3$) and corresponding critical frequency ($\omega_{cr} = \omega b^2 / \pi^2 \sqrt{\rho / E_2 h^2}$) for 8 layered constant stiffness and variable stiffness square composite laminates for different boundary conditions ($a/h = 100$).	119
Table 8.3.2.	Critical flutter load ($\lambda_{cr} = \lambda a^3 / E_2 h^3$) for isotropic, constant stiffness and variable stiffness composite plate under combined in-plane compression and aerodynamic pressure for two different boundary conditions.	120
Table 8.3.3.	Critical flutter load ($\lambda_{cr} = \lambda a^3 / E_2 h^3$) for isotropic, constant stiffness and variable stiffness composite plate under combined in-plane shear (positive and negative) and aerodynamic pressure for two different boundary conditions.	121
Table 8.4.1.	Critical aerodynamic pressure ($\lambda_{cr} = \lambda a^3 / E_2 h^3$) and corresponding critical frequency ($\varpi = \omega b^2 / \pi^2 \sqrt{\rho / E_2 h^2}$) for 8 layered constant stiffness and variable stiffness symmetric ($\alpha = \beta = 73.3^0$) and un-symmetric ($\alpha = 63.435^0$, $\beta = 84.29^0$) trapezoidal composite laminates for different boundary conditions ($a = b$, $a/h = 100$, $c/a = 0.4$).	123
Table 8.4.2.	Critical aerodynamic pressure ($\lambda_{cr} = \lambda a^3 / E_2 h^3$) for isotropic and composite un-symmetric ($\alpha = 63.435^0$, $\beta = 84.29^0$) trapezoidal cantilever plate ($a = b$, $a/h = 100$, $c/a = 0.4$).	123

NOMENCLATURE AND ABBREVIATIONS

English Notations

a	:	Length of the panel
b	:	Width of the panel
u_0	:	In-plane displacement along X-direction
v_0	:	In-plane displacement along Y-direction
w_0	:	In-plane displacement along Z-direction
A	:	Extensional stiffness coefficient
B	:	Bending-extensional stiffness coefficient
D	:	Bending stiffness coefficient
S	:	shear stiffness coefficient
N_i	:	Shape function corresponding to ' <i>i-th</i> ' node
E	:	Young's modulus
F	:	Load vector
G	:	Shear modulus
h	:	Thickness
$[M]$:	Mass matrix
$[K_L]$:	Linear stiffness
$[K_{NL}]$:	Nonlinear stiffness
$[K_G]$:	Geometric stiffness matrix
\bar{N}_{xy}	:	In-plane edge shear
$\bar{N}_{xx} / \bar{N}_{yy}$:	In-plane edge compression
C	:	Parametric coefficient matrix
N_{cr}	:	Critical buckling load
N_{xx}^F	:	Compressive follower force
N_{xy}^F	:	Shear follower force
K_{NC}	:	Non-conservative load matrix
g_T	:	Aerodynamic damping parameter
U_a	:	Air flow velocity

$[A_a]$:	Aerodynamic load matrix
M	:	Mach number

Greek Notations

θ	:	Slope of curvilinear fibre
φ_x	:	Rotation of the normal about Y axis
φ_y	:	Rotation of the normal about X axis
ε	:	Strain
γ	:	Shear strain
δ	:	Degrees of freedom vector
κ	:	Curvature
γ^{AS}	:	Assumed shear strain
β	:	Periodic in-plane load
β_s	:	Static in-plane load
ϕ	:	Modal matrix
ξ_m	:	Amplitude of the m -th vibration mode
Ω	:	Excitation frequency
ω	:	Natural frequency
σ	:	Detuning parameter
α	:	Non-conservativeness parameter
λ_{cr}	:	Flutter load
ω_R	:	Real frequency
ω_I	:	Imaginary frequency
λ	:	Aerodynamic pressure parameter
ρ_a	:	Density of air
ρ	:	Density of plate
ϖ	:	Non-dimensional natural frequency
μ	:	Poisson's ratio

Abbreviations

FEM	:	Finite Element Method
FSDT	:	First Order Shear Deformation Theory
CSCL	:	Constant Stiffness Composite Laminates
VSCL	:	Variable Stiffness Composite Laminates
MITC	:	Mixed Interpolation of Tensorial Components
MMS	:	Method of Multiple Scales
C	:	Clamped
F	:	Free
S	:	Simply supported
IPBC	:	Inplane boundary condition
DIRS	:	Dynamic instability regions